

Unification theory of instabilities of visco-diffusive swirling flows

Oleg N. Kirillov*

Northumbria University, Newcastle upon Tyne, NE1 8ST, United Kingdom

Innocent Mutabazi

Laboratoire Ondes et Milieux Complexes, UMR-6294 CNRS,
Université Le Havre Normandie, Normandie Université,
53 Rue de Prony, 76058 Le Havre Cédex, France

(Dated: July 3, 2024)

A universal theoretical model of instabilities in swirling flows occurring in nature or industrial processes is developed. This model encompasses various open and confined flows including spiral Couette flow, spiral Poiseuille flow, and baroclinic Couette flow, which results from the combination of differential rotation and baroclinic convection due to radial heating and natural gravity. Utilizing short-wavelength local analysis, the model generalizes previous results from numerical simulations and linear stability analysis of specific flows. A general criterion for instability is derived, incorporating viscous dissipation and thermal diffusion, thereby extending and uniting existing criteria (Rayleigh for centrifugally-driven flows, Lüdweg-Eckhoff-Leibovich-Stewartson for isothermal spiraling flows, and Goldreich-Schubert-Fricke for non-isothermal azimuthal flows).

Swirling flows induced by the combination of rotation and shear in orthogonal directions are ubiquitous in various natural phenomena, such as tornadoes and tropical cyclones [1, 2], meandering rivers [3], vortex rings with swirl [4], geophysical and astrophysical flows [5], and recently discovered magnetic tornadoes in the solar atmosphere [6]. These flows also occur in trailing vortices of aircraft wingtips [7–10] and in branching junctions of everyday piping systems and physiological flows [11], where identifying instabilities that lead to vortex breakdown is of paramount importance [12]. Swirling flows are present in industrial processes, such as filtration or purification of wastewater [13], isotope separation through centrifugation [14], and oil-drilling systems [15]. They are also characteristic of convective flows with rotation [16], associated with cooling or lubrication of rotating machinery [17], crystal growth [18], and solidification of metals [19].

From a hydrodynamic perspective, swirling flow consists of azimuthal and axial velocity components in either open or confined geometries. The unbounded geometry is typical of swirling jets in natural phenomena, while the bounded one is common in engineering. A convenient setup to study swirling flows, both theoretically and experimentally, confines fluid in a cylindrical annulus with differentially rotating cylinders, creating the classical circular Couette-Taylor flow. The axial component in this setup can be induced by an external pressure gradient, as in Spiral Poiseuille flow (SPF) [20–22], by sliding inner cylinder, as in Spiral Couette flow (SCF) [23–26], or by a radial temperature gradient, as in baroclinic Couette flow (BCF) [27–29]. While SPF and SCF are stationary solutions to the Navier-Stokes equations, BCF is a stationary solution to the Navier-Stokes equations coupled with the energy equation via buoyancy terms.

In the absence of axial flow and a radial temperature gradient, a differentially rotating azimuthal flow of inviscid incompressible fluid becomes centrifugally unstable if it meets the Rayleigh criterion, which states that angular momentum must decrease outward for instability to occur [30]. Including viscosity only slightly reduces the instability domain defined by this result [30]. However, a radial temperature gradient and thermal diffusion can destabilize Rayleigh-stable flows, such as quasi-Keplerian ones [31, 32]. This phenomenon is described by the visco-diffusive extension of Rayleigh’s criterion, known as the Goldreich-Schubert-Fricke (GSF) instability condition, applied to non-isothermal differentially rotating azimuthal flows [33]. The GSF instability may significantly influence angular momentum transport in stellar radiation zones and astrophysical discs, driving turbulence and stirring solids in protoplanetary disc regions that are stable to magnetorotational instability [34].

In the absence of azimuthal rotation, axial flows in a cylindrical annulus are subject to wall-driven shear instabilities. Annular Poiseuille flow becomes linearly unstable above a critical axial Reynolds number for all $0 < \eta \leq 1$, where η is the ratio of the inner to outer cylinder radii [35]. For sliding Couette flow, the critical Reynolds number is finite for $0 < \eta < 0.1415$ and infinite otherwise, with the unstable mode being axisymmetric [36]. Baroclinic convection in a vertical annulus with a horizontal temperature gradient becomes linearly unstable to predominantly axisymmetric perturbations above a finite axial Grashof number for $0.01 \leq \eta \leq 0.99$ when the Prandtl number, the ratio of viscosity to thermal diffusivity, is between 1 and 30 [37, 38].

In contrast, the swirling flows can become unstable due to both centrifugally-driven and shear-driven perturbations. The competition between these destabilizing mechanisms leads to a rich variety of flow patterns and bifurcations, as documented in the scattered experimental, theoretical, and numerical studies [20–29].

* author for correspondence : oleg.kirillov@northumbria.ac.uk

An unusual phenomenon discovered in swirling flows, is the zeroth order discontinuity in the critical Couette-flow Reynolds number of the rotating inner cylinder in the Rayleigh-stable regime. Surprisingly, this discontinuity occurs in both spiral Poiseuille [21] and spiral Couette [26] isothermal flows, despite their different shear profiles. The common mathematical reason for this phenomenon is a *folding* in the critical surface that determines the neutral stability boundary in the space of the two azimuthal Reynolds numbers and the axial Reynolds number, defined by the sliding speed of the inner cylinder for SCF and by the mean velocity of the axial flow for SPF. This folding reflects the competition between centrifugal and shear instability mechanisms in swirling flows. Detecting the folding in [21, 26] required developing a *specifically tailored numerical scheme*.

The only *analytical* stability criterion in this context is available for isothermal inviscid incompressible swirling flows. It is the extension of Rayleigh's criterion, derived via a global modal approach by Lüdewig [23] for SCF in the narrow gap limit and by Leibovich and Stewartson [10] for swirling jets. Eckhoff [9] arrived at the same criterion using the local geometrical optics approach [4], deriving instability conditions by tracing a localized wave packet along the streamlines of the helical base flow. Leblanc and Le Duc [39] established a formal equivalence between the local and global approaches to the Lüdewig-Eckhoff-Leibovich-Stewartson (LELS) criterion in the limit of large wavenumbers. However, the LELS criterion, limited to inviscid flows, cannot describe the folded neutral stability surface of SCF and SPF, nor can it be applied to non-isothermal swirling flows. A theory unifying these phenomena has yet to be formulated.

This Letter presents a general theoretical framework for investigating the stability of both viscous isothermal and visco-diffusive non-isothermal swirling flows using the local geometrical optics stability analysis pioneered in the hydrodynamics of inviscid flows [4, 9, 40] and recently extended to visco-diffusive flows [31, 41, 42]. We apply it to the helical stationary solutions of the Navier-Stokes equations coupled with the energy equation in the Boussinesq approximation, which, depending on the boundary conditions, can represent SCF, SPF, or BCF.

We establish that the neutral stability curves in the plane of the two Reynolds numbers for azimuthal and axial velocities form families with a consistent *envelope*, regardless of whether they are parameterized by the azimuthal or axial wavenumber. Since the axial wavenumber can take arbitrary real value, this envelope defines the boundary of the union of individual instability domains for specific wavenumbers, providing a comprehensive instability criterion that includes the Rayleigh, GSF, and LELS criteria as special cases.

We find that the envelope, and thus the instability domain, splits during the transition from Rayleigh-unstable to Rayleigh-stable flows. For Rayleigh-stable flows, as the azimuthal Reynolds number approaches infinity, an asymptotic line to the envelope represents the inviscid

LELS criterion for the isothermal flows and yields an analytical expression for the new united LELS-GSF criterion for the non-isothermal flows. In the isothermal case, we find a compact closed-form expression for the envelope, generalizing the inviscid LELS criterion to viscous swirling flows and covering the full range of azimuthal Reynolds numbers from zero to infinity. This extension broadens the criterion's applicability to previously inaccessible, practically important situations and offers an exact analytical expression for the folded neutral stability surface, *universal for all isothermal swirling flows*.

We consider an incompressible Newtonian fluid with density ρ , thermal expansion coefficient α , kinematic viscosity ν , and thermal diffusivity κ . This fluid is confined within an infinitely long cylindrical annulus with a gap width $d = R_2 - R_1$, where R_1 is the radius of the inner cylinder at temperature T_1 , rotating with angular velocity Ω_1 , and R_2 is the radius of the outer cylinder at temperature $T_2 = T_1 - \Delta T$, rotating with angular velocity Ω_2 . We denote $\eta = R_1/R_2$ and $\mu = \Omega_2/\Omega_1$. The system is subjected to a uniform gravity field with acceleration g along the Z -axis of the cylindrical coordinates (R, φ, Z) , which aligns with the common rotation axis of the cylinders.

We assume the base flow to be helical, with $V_0 = \Omega_1 R_1$ and W_0 being the characteristic azimuthal and axial velocities, respectively. Choosing V_0 as the velocity scale, d as the length scale, d/V_0 as the time scale, and ρV_0^2 as the pressure scale, and applying the Boussinesq-Oberbeck approximation—which assumes all fluid properties are constant except for the density, which varies linearly with temperature in the driving forces—we write the dimensionless governing equations:

$$\begin{aligned} \nabla \cdot \mathbf{u} &= 0, \\ \frac{d\mathbf{u}}{dt} + \nabla p - \frac{1}{Re} \nabla^2 \mathbf{u} + \left(\gamma \frac{v^2}{r} \mathbf{e}_r - Ri \mathbf{e}_z \right) \theta &= 0, \\ \frac{d\theta}{dt} - \frac{1}{RePr} \nabla^2 \theta &= 0, \end{aligned} \quad (1)$$

where p and $\mathbf{u} = (u, v, w)$ are the dimensionless pressure and velocity field, respectively, $\theta = \frac{T-T_2}{\Delta T}$ is the temperature deviation, $\frac{d}{dt} = \frac{\partial}{\partial t} + \mathbf{u} \cdot \nabla$, $r = \frac{R}{d}$, and $z = \frac{Z}{d}$.

The dimensionless parameters in Eq. (1) are

$$Re = \frac{V_0 d}{\nu}, \quad Ri = \frac{W_T}{V_0 Re}, \quad Pr = \frac{\nu}{\kappa}, \quad (2)$$

where Re is the Reynolds number associated with the rotation of the inner cylinder, Pr is the Prandtl number, and Ri is the Richardson number defined using the characteristic thermal velocity $W_T = \frac{\gamma g d^2}{\nu}$ and $\gamma = \alpha \Delta T$, with $\gamma > 0$ for outward heating ($T_1 > T_2$).

In a cylindrical annulus with infinite aspect ratio, the base flow state is stationary and axially invariant. Its two-component dimensionless velocity field is $\mathbf{u}_B(r) = (0, V(r), S^{-1}W(r))$, where $S = \frac{V_0}{W_0}$ is the swirl parameter [25, 28]. The temperature $\theta_B(r) = \Theta(r)$ depends only on the radial coordinate r , while the pressure is given by $p_B(r, z) = P_1(r) + zP_2$ [25, 28].

To produce the BCF, we set $W_0 = W_T$ and impose the boundary conditions: $V(r_1) = 1$, $V(r_2) = \mu/\eta$, $W(r_{1,2}) = 0$, and $\Theta(r_1) = 1$, $\Theta(r_2) = 0$, where $r_1 = \frac{\eta}{1-\eta}$ and $r_2 = \frac{1}{1-\eta}$. The azimuthal velocity profile and the temperature profile of BCF are given by:

$$V(r) = Ar + \frac{B}{r}, \quad \Theta(r) = \frac{\ln[(1-\eta)r]}{\ln \eta} \quad (3)$$

with $A = \frac{\mu-\eta^2}{\eta(1+\eta)}$ and $B = \frac{\eta}{1+\eta} \frac{1-\mu}{(1-\eta)^2}$. In addition to the two integration constants fixed by the boundary conditions, the axial profile $W(r)$ of BCF depends on the gradient P_2 , which is determined by the condition of zero axial mass flux $\int_{r_1}^{r_2} rW(r)dr = 0$, and reads [28]:

$$W(r) = C \left[(r_2^2 - r_1^2) \frac{\ln(r/r_2)}{\ln \eta} + r^2 - r_2^2 \right] - (r^2 - r_1^2) \frac{\ln(r/r_2)}{4 \ln \eta},$$

$$C = \frac{1}{16} \frac{(1-3\eta^2)(1-\eta^2) - 4\eta^4 \ln \eta}{(1-\eta^2)^2 + (1-\eta^4) \ln \eta}. \quad (4)$$

Introducing the axial Reynolds number, $Re_z = \frac{W_0 d}{\nu}$, we observe that setting $W_0 = W_T$ results in $Re_z = Gr$, the Grashof number, characterizing the magnitude of the baroclinic flow. Hence, $Ri = \frac{Gr}{Re^2}$ and $S = \frac{Re}{Gr}$.

To test the stability of the base flow (3), (4), we introduce small three-dimensional perturbations (\mathbf{u}' , p' , θ') and linearize the nonlinear equations (1) about the base BCF state. Using a small parameter $0 < \epsilon \ll 1$ and assuming $Re \sim \epsilon^{-2}$ as proposed by [42], we represent the perturbations as asymptotic expansions [4, 9, 40, 41]:

$$\begin{aligned} \mathbf{u}' &= (\mathbf{u}^{(0)}(\mathbf{x}, t) + \epsilon \mathbf{u}^{(1)}(\mathbf{x}, t)) e^{\frac{i\Phi(\mathbf{x}, t)}{\epsilon}} + \epsilon \mathbf{u}^{(r)}(\mathbf{x}, t, \epsilon), \\ \theta' &= (\theta^{(0)}(\mathbf{x}, t) + \epsilon \theta^{(1)}(\mathbf{x}, t)) e^{\frac{i\Phi(\mathbf{x}, t)}{\epsilon}} + \epsilon \theta^{(r)}(\mathbf{x}, t, \epsilon), \\ p' &= (p^{(0)}(\mathbf{x}, t) + \epsilon p^{(1)}(\mathbf{x}, t)) e^{\frac{i\Phi(\mathbf{x}, t)}{\epsilon}} + \epsilon p^{(r)}(\mathbf{x}, t, \epsilon), \end{aligned} \quad (5)$$

where $i = \sqrt{-1}$ and $\mathbf{u}^{(r)}$, $p^{(r)}$, $\theta^{(r)}$ are uniformly bounded in ϵ . By substituting (5) into the linearized equations and

$$\mathcal{H} = \begin{pmatrix} -\frac{DW}{SRO} \frac{k_r k_z}{|\mathbf{k}|^2} - \frac{|\mathbf{k}|^2}{Re} & 2\Omega(1-\gamma\Theta) \left(1 - \frac{k_r^2}{|\mathbf{k}|^2}\right) & -\left(r\gamma\Omega^2 \left(1 - \frac{k_r^2}{|\mathbf{k}|^2}\right) + Ri \frac{k_r k_z}{|\mathbf{k}|^2}\right) \\ -2\Omega \left(Ro + \frac{k_r^2 + k_z^2}{|\mathbf{k}|^2}\right) & (1-\gamma\Theta) \frac{DW}{SRO} \frac{k_r k_z}{|\mathbf{k}|^2} - \frac{|\mathbf{k}|^2}{Re} & -\left(r\gamma\Omega^2 - Ri \frac{k_z}{k_r}\right) \frac{1}{2\Omega} \frac{DW}{SRO} \frac{k_r k_z}{|\mathbf{k}|^2} \\ -D\Theta & 0 & \frac{|\mathbf{k}|^2}{Re} \frac{Pr-1}{Pr} - \frac{|\mathbf{k}|^2}{Re} \end{pmatrix}. \quad (9)$$

The dispersion relation defined by (9) is a cubic polynomial equation $\lambda^3 + a_2 \lambda^2 + a_1 \lambda + a_0 = 0$ with real coefficients. Therefore, the stability conditions of the base flow ($\sigma < 0$) are defined by the Lienard-Chipart stability

collecting all terms with the same powers of ϵ , we obtain a hierarchical system of equations in ϵ . At orders ϵ^{-1} and ϵ^0 , the pressure terms can be eliminated.

This simplification yields equations in the stationary frame for the amplitudes $\mathbf{u}^{(0)}$, $\theta^{(0)}$ of the localized wave packet moving along the streamlines of the base flow:

$$\begin{aligned} \frac{d\mathbf{u}^{(0)}}{dt} + \frac{|\mathbf{k}|^2}{Re} \mathbf{u}^{(0)} &= -\left(\mathcal{I} - \frac{\mathbf{k}\mathbf{k}^T}{|\mathbf{k}|^2}\right) \left(\gamma \frac{V^2}{r} \mathbf{e}_r - Ri \mathbf{e}_z\right) \theta^{(0)} \\ &\quad - \left(\mathcal{I} - 2 \frac{\mathbf{k}\mathbf{k}^T}{|\mathbf{k}|^2}\right) \mathcal{U} \mathbf{u}^{(0)} - 2\gamma\Theta\Omega \left(\mathcal{I} - \frac{\mathbf{k}\mathbf{k}^T}{|\mathbf{k}|^2}\right) \mathbf{e}_r \mathbf{e}_\varphi^T \mathbf{u}^{(0)}, \\ \frac{d\theta^{(0)}}{dt} + \frac{|\mathbf{k}|^2}{RePr} \theta^{(0)} &= -(\nabla\Theta)^T \mathbf{u}^{(0)}, \end{aligned} \quad (6)$$

where the wavevector $\mathbf{k} = \frac{\nabla\Phi}{\epsilon}$ satisfies the equation

$$\frac{d\mathbf{k}}{dt} = -\mathcal{U}^T \mathbf{k}, \quad \mathcal{U} = \begin{pmatrix} 0 & -\Omega & 0 \\ \Omega(1+2Ro) & 0 & 0 \\ S^{-1}DW & 0 & 0 \end{pmatrix} \quad (7)$$

with \mathcal{I} the identity matrix, $\mathbf{k} \cdot \mathbf{u}^{(0)} = 0$, $\frac{d}{dt} = \frac{\partial}{\partial t} + \mathbf{u}_B \cdot \nabla$, $D = \frac{d}{dr}$, $\Omega = \frac{V}{r}$, and the Rossby number $Ro = \frac{rD\Omega}{2\Omega}$.

In the frame of the wave packet, rotating about the vertical axis with the angular velocity Ω , the wavevector $\mathbf{k} = (k_r, k_\varphi, k_z)$ is time-independent and the amplitude equations (6) are autonomous, provided that [2, 9, 10]

$$k_\varphi = -\overline{DW} k_z, \quad \overline{DW} = \frac{DW}{2\Omega Ro S}. \quad (8)$$

Thus, the most unstable and exponentially growing 3D perturbations in swirling flows exhibit helical symmetry [2]. This means they are invariant along the circular helices with the pitch $2\pi r \overline{DW}$ [8–10].

Assuming $\mathbf{u}^{(0)}$, $\theta^{(0)} \sim e^{st+im\varphi+ik_z z}$ in (6), where $s = \sigma + i\omega$ is the complex growth rate, and $m = k_\varphi r$ and k_z are the integer azimuthal and real axial wavenumbers of the perturbations, and taking into account (8), we obtain the dispersion relation $\det(\mathcal{H} - \lambda\mathcal{I}) = 0$, where $|\mathbf{k}|^2 = k_r^2 + k_z^2 \left[1 + \overline{DW}^2\right]$, $\lambda = \sigma + i(\omega + m\Omega + k_z W/S)$, and

criterion as the following three inequalities [31]:

$$a_0 > 0, \quad a_2 > 0, \quad a_0(a_1 a_2 - a_0) > 0. \quad (10)$$

The condition

$$\begin{aligned} a_0 &= \frac{D\Theta DW}{SRO} \frac{k_z^2}{|\mathbf{k}|^2} Ri(1-\gamma\Theta) - \frac{k_r k_z}{|\mathbf{k}|^2} \frac{|\mathbf{k}|^2}{Re} Ri D\Theta + \frac{|\mathbf{k}|^2 \Omega^2}{Re Pr} \left(1 - \frac{k_r^2}{|\mathbf{k}|^2}\right) \left\{4 \left[Ro + \frac{k_r^2 + k_z^2}{|\mathbf{k}|^2}\right] (1-\gamma\Theta) - \gamma r D\Theta Pr\right\} \\ &\quad + \frac{|\mathbf{k}|^2}{Re Pr} \left(\frac{|\mathbf{k}|^2}{Re} - \frac{k_r k_z}{|\mathbf{k}|^2} \frac{DW}{SRO} (1-\gamma\Theta)\right) \left(\frac{|\mathbf{k}|^2}{Re} + \frac{k_r k_z}{|\mathbf{k}|^2} \frac{DW}{SRO}\right) = 0, \end{aligned} \quad (11)$$

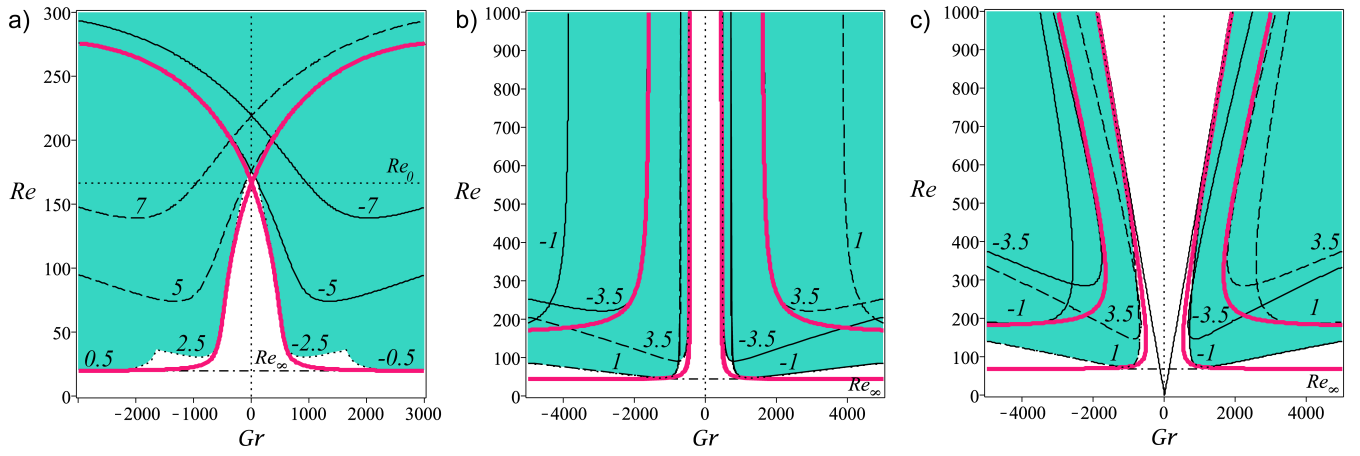


FIG. 1. Neutral stability curves (11) parameterized by k_z , with their envelope (red, thick) for the non-isothermal BCF. Parameters are $Pr = 5.5$, $\gamma = 0.0004$, $k_r = 1.7\pi$, and $\eta = 0.8$ for the three different μ : (a) Rayleigh unstable, $\mu = 0$; (b) modified Rayleigh line, $\mu = \mu_R \approx 0.63935$ (from (13)); and (c) Rayleigh stable, $\mu = 0.8$. The envelope at $Gr = 0$ in (a) gives $Re_0 \approx 166.8$ from (12). Shaded regions are instability domains for specific k_z . Solid oblique straight lines in (c) represent the united LELS-GSF criterion (14). All computations for the BCF are performed at the mean geometric radius $r = \sqrt{r_1 r_2}$.

yields $\lambda = 0$, corresponding to marginally stable modes with the frequency $\omega = -m\Omega - k_z W/S$, which are inclined on the cylindrical surface of radius r and have azimuthal and axial phase velocities $c_\varphi = -\Omega r$ and $c_z = -k_z W/S$. In view of $Ri = \frac{1}{ReS}$, the limit $S \rightarrow \infty$ of (11) retrieves the critical value of Re for stationary modes of the thermal convection induced by centrifugal buoyancy in the differentially rotating cylindrical annulus [31].

In general, (11) defines a family of marginal stability curves in the (Gr, Re) -plane, parameterized by the axial wavenumber k_z (or m via the relation (8)). The inequality $a_0 < 0$ then delineates the individual instability domains for a given k_z (or m), as shown in Fig. 1.

Our first key finding, overlooked in previous works, is that the individual marginal stability curves of the BCF have an envelope determined by computing the discriminant of (11), treated as a polynomial in k_z or m [43].

This envelope, independent of the chosen parameterization, separates the domain of unstable modes from the stability zone. It consists of two distinct symmetric curves that can intersect at $Gr = 0$ and $Re = Re_0$, where

$$Re_0 = \frac{3\sqrt{3}k_r^2}{2\Omega} \frac{1}{\sqrt{rD\Theta\gamma Pr - 4(1+Ro)(1-\gamma\Theta)}}, \quad (12)$$

as shown in Fig. 1(a). The requirement for the radicand in (12) to be positive defines the modified Rayleigh line for non-isothermal flows:

$$Ro_R = -1 + \frac{rD\Theta\gamma Pr}{4(1-\gamma\Theta)} = -1 + \frac{1}{4}\gamma Pr rD\Theta + O(\gamma^2). \quad (13)$$

While intersecting for $Ro < Ro_R$, the envelope branches have vertical asymptotes at the modified Rayleigh line (13), delimiting the zone where no instability modes can be obtained, Fig. 1(b). For $Ro > Ro_R$ the

asymptotes are inclined, placing the instability domains within the half-planes defined by the asymptotes to the external branch, shown by oblique lines in Fig. 1(c):

$$\frac{N_\Omega^2}{\Omega^2}(1-\gamma\Theta) + Pr \frac{N^2}{\Omega^2} < \frac{(\overline{DW}(2-\gamma\Theta) - \frac{PrD\Theta}{2k_z^2\Omega S})^2}{1 + \overline{DW}^2}. \quad (14)$$

Here $N_\Omega^2 = 4(1+Ro)\Omega^2$ is the Rayleigh discriminant, $N^2 = -\gamma\Omega^2 rD\Theta$ is the square of the centrifugal Brünt-Väissälä frequency [31], and $S = Gr/Re$.

The inequality (14) yields the inviscid LELS criterion

$$\frac{N_\Omega^2}{\Omega^2} - \frac{4\overline{DW}^2}{1 + \overline{DW}^2} < 0 \quad (15)$$

in the isothermal case $\Theta \equiv 0$ [10], and the GSF criterion

$$N_\Omega^2(1-\gamma\Theta) + PrN^2 < 0 \quad (16)$$

in the limit of azimuthal flow $S \rightarrow \infty$ [31, 33]. Thus, (14) is a new unified LELS-GSF criterion for viscous and thermodiffusive swirling flows (accounting for Pr).

The envelope in Fig. 1 closely matches the critical states curve from both linear stability analysis and experiments [29]. The envelope, unlike individual neutral stability curves, has a horizontal asymptote at $Re = Re_\infty$ as $|Gr| \rightarrow \infty$. This explains the seemingly smooth and nearly Gr -independent stability boundary observed in [29] for $\mu = 0$, although this boundary is actually piecewise smooth, with each neutral stability curve touching the common envelope, which flattens at large $|Gr|$ where shear instability dominates. Despite the Rayleigh-Fjörtoft shear instability mechanism due to an inflection point in the axial velocity profile [44] leading to axisymmetric perturbations [37], rotation ensures that the critical modes of the BCF are three-dimensional [45].

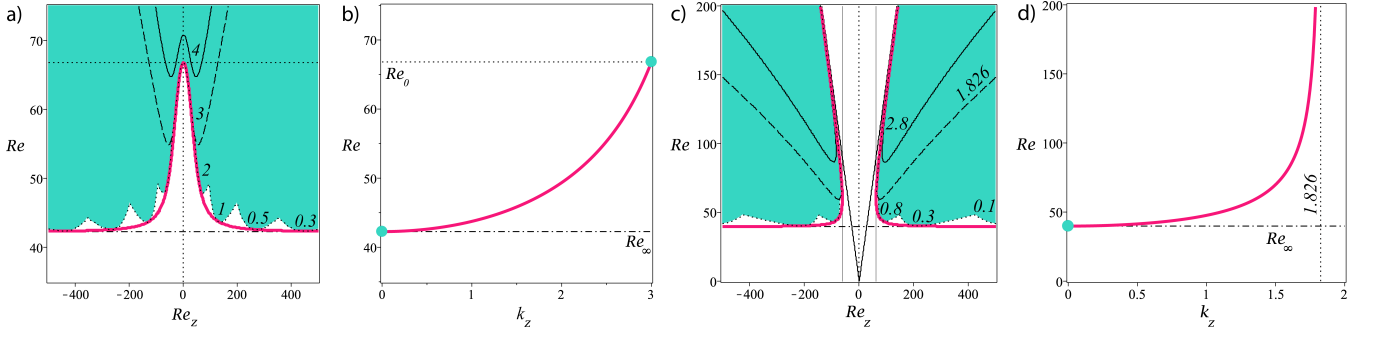


FIG. 2. (a, c) Neutral stability curves (11) in the (Re_z, Re) -plane, parameterized by k_z . The thick red curves show their envelope (18) for the isothermal enclosed SCF (19) with $\eta = 0.4$ and $k_r = 3\sqrt{2}$. Panels (a, b) represent $\mu = 0$, and panels (c, d) represent $\mu = 0.5$. The black dashed curves correspond to the terminal $k_z = \frac{\sqrt{2}}{2}k_r = 3$ in (a) and the terminal $k_z = \frac{\sqrt{-2Ro}}{2}k_r \approx 1.826$ in (c). The oblique black solid lines in (c) indicate the inviscid LELS criterion (18). Vertical solid lines in (c) show $\pm Re_z^{\min}$ (21). (b,d) Variation of k_z from 0 to the terminal value according to (22) as Re increases from Re_∞ (dot-dashed line) to (b) Re_0 (dotted line) or (d) to infinity. All computations for the SCF are performed at the mean geometric radius $r = \sqrt{r_1 r_2}$.

Figure 1, in conjunction with relation (8), demonstrates how the envelope selects the critical modes. The lower left branch of the envelope corresponds to the left spiral modes ($k_z > 0$, $m > 0$), while the lower right branch corresponds to the right spiral modes ($k_z < 0$, $m > 0$). This is consistent with findings in [28].

Computing tangent lines to the envelope in the (Gr, Re) -plane at the intersection point (12) in the Rayleigh-unstable regime ($Ro < Ro_R$) yields:

$$\frac{Re}{Re_0} = 1 \pm \sqrt{2} \frac{2D\Theta Pr Ro - 3DW\Theta\gamma k_r^2}{27Rok_r^4} Gr. \quad (17)$$

This indicates that the temperature gradient is responsible for the existence of two branches that should merge into a single curve for isothermal Rayleigh-unstable flows.

Setting $\gamma = 0$ and $Ri = 0$ in (11), we greatly simplify the equation in the isothermal case. This leads to *our second key finding*, which is the simple analytical expression for the envelope of the neutral stability curves for isothermal swirling flows:

$$E(Re_z, Re) = \frac{N_\Omega^2}{\Omega^2} - \frac{4\overline{DW}^2}{1 + \overline{DW}^2} + \frac{27}{4\Omega^2} \frac{k_r^4}{Re^2} = 0. \quad (18)$$

Then, the swirl parameter $S = \frac{Re}{Re_z}$ in (8), (11), and (18) is redefined via the axial Reynolds number $Re_z = \frac{W_0 d}{\nu}$, where W_0 is the appropriate axial flow velocity.

For example, in the enclosed SCF base flow $W_0 = W_1$, the sliding speed of the inner cylinder, the dimensionless axial velocity $W(r)$ is [25, 26]:

$$W(r) = \frac{(2\eta^2 \ln \eta - \eta^2 + 1)(r^2 - r_2^2) - (\eta + 1)^2 \ln(r/r_2)}{((\eta^2 + 1) \ln \eta - \eta^2 + 1)(\eta + 1)(\eta - 1)^{-1}}, \quad (19)$$

while $V(r)$ is defined by (3). The individual neutral stability curves (11) and their envelope (18) for SCF are shown in the (Re_z, Re) -plane in Fig. 2. For Rayleigh-unstable flows ($N_\Omega^2 < 0$ or $Ro < -1$), (18) is a single

curve confirming our hypothesis based on (17). The envelope has a maximum $Re = Re_0$ when $Re_z = 0$ and a horizontal asymptote $Re = Re_\infty$ as $|Re_z| \rightarrow \infty$, where:

$$Re_0 = \frac{3\sqrt{3}k_r^2}{4\Omega\sqrt{-Ro-1}}, \quad Re_\infty = \frac{3\sqrt{3}k_r^2}{4\Omega\sqrt{-Ro}}. \quad (20)$$

As $Ro \rightarrow -1$, $Re_0 \rightarrow \infty$, and for Rayleigh-stable flows ($-1 < Ro < 0$), the envelope splits into two curves, each with vertical tangents at $Re_z = \pm Re_z^{\min}$, where

$$Re_z^{\min} = \frac{3}{2} \frac{\sqrt{3}k_r^2}{DW} (1 + \sqrt{Ro+1}) \quad (21)$$

is the threshold axial velocity needed to destabilize Rayleigh-stable isothermal azimuthal flows.

The inequality $E(Re_z, Re) < 0$ is the viscous extension of the LELS criterion (15). In Fig. 2, criterion (15) is represented for Rayleigh-stable flows by the oblique solid lines touching the upper parts of the envelope (18) as $Re \rightarrow \infty$. While (15) does not apply to Rayleigh-unstable flows, its viscous extension defines the stability boundary in this case, as given by the envelope (18). Setting $\overline{DW} = 0$ in (18) retrieves the stability boundary for isothermal Couette-Taylor flow found in [30].

The explicit expressions (18) and (20) available for isothermal swirling flows allow us to analytically determine the variation of k_z along the stability boundary:

$$|k_z|(Re) = k_r \frac{\sqrt{2}}{2} \sqrt{\frac{1 - Re_\infty^2/Re^2}{1 - Re_\infty^2/Re_0^2}}. \quad (22)$$

Thus, $|k_z| \rightarrow 0$ as $Re \rightarrow Re_\infty$ and reaches its terminal value $\frac{\sqrt{2}}{2}k_r$ at $Re = Re_0$ for Rayleigh-unstable flows, Fig. 2(b), and $\frac{\sqrt{-2Ro}}{2}k_r$ as $Re \rightarrow \infty$ for Rayleigh-stable flows, Fig. 2(d), agreeing with numerical studies [23–26].

The envelope equation (18) is *universal* for all isothermal swirling flows. For swirling flows between differentially rotating cylinders, we express $\mu = \Omega_2/\Omega_1$ in

$\Omega = V/r$ (see (3)) using the Reynolds numbers of the inner ($Re = \frac{R_1 \Omega_1 d}{\nu}$) and outer ($Re_2 = \frac{R_2 \Omega_2 d}{\nu}$) cylinders as $\mu = \eta \frac{Re_2}{Re}$ [21, 26]. This reparameterization of Eq. (18) returns the neutral stability surface in (Re_z, Re_2, Re) -space, as shown in Fig. 3 for the enclosed SCF.

At $Re_z = 0$, the surface yields the neutral stability curve of the Couette-Taylor flow [30]. However, as Re_z increases, the critical Re decreases until it abruptly falls, as shown in Fig. 3, due to a fold first observed numerically for SCF in [26] and then for SPF in [21], despite its different axial shear profile. The apparent paradox, reminding the Velikhov-Chandrasekhar paradox in magnetohydrodynamics [46], is explained by the universality of (18) for isothermal swirling flows.

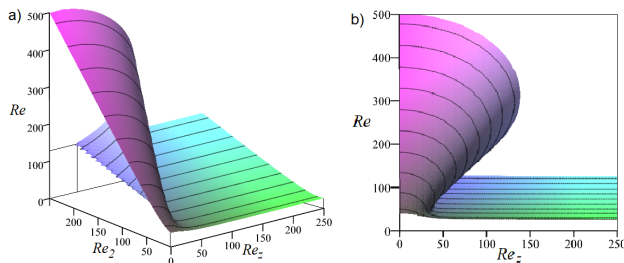


FIG. 3. For the SCF (19) with $k_r = \pi$ and $\eta = 0.5$: (a) The folded surface of the envelope (18) in the (Re_z, Re_2, Re) -space and (b) its projection onto the (Re_z, Re) -plane.

In conclusion, by employing local geometrical optics stability analysis adapted to visco-diffusive flows, we derived a novel explicit instability criterion for viscous swirling flows. This generalizes the inviscid Lüdwig-Eckhoff-Leibovich-Stewartson (LELS) stability condition and introduces a new analytical instability criterion for non-isothermal visco-diffusive swirling flows, uniting the LELS and the Goldreich-Schubert-Fricke criteria.

Our advancement stems from an observation overlooked in previous research: the neutral stability curves in these problems possess an envelope, which we have analytically determined using the connection between envelopes and polynomial discriminants. Our analytical results offer a general theory of instabilities across a wide range of swirling flows.

Specifically, our expression for the folded neutral stability surface of isothermal swirling flows elucidates the universal occurrence of zero-order discontinuities in the azimuthal Reynolds number across flows with various shear distributions, highlighting the interplay between shear and centrifugal instability mechanisms.

ACKNOWLEDGMENTS

This work was supported by the French Space Agency (CNES) and the ANR Programme d'Investissements d'Avenir LABEX EMC³ through the INFEMA project.

-
- [1] K.A. Emanuel, *100 Years of Progress in Tropical Cyclone Research*, American Meteorological Society, 2018.
 - [2] K.A. Emanuel, *J. Fluid Mech.* **145**, 235 (1984).
 - [3] S.W. Park and J. Ahn, *Smart Water* **4**, 4 (2019).
 - [4] A. Lifschitz and E. Hameiri, *Comm. Pure Appl. Math.* **46**, 1379 (1993).
 - [5] E. Knobloch and H.C. Spruit, *A&A* **113**, 261 (1982); F.H. Busse and W. Pesch, *Geophys. Astrophys. Fluid Dyn.* **100**, 139 (2006); J.M. Lopez, F. Marques, and M. Avila, *J. Fluid Mech.* **737**, 56 (2013).
 - [6] S. Wedemeyer-Böhm et al., *Nature* **486**, 505-508 (2012); A.D. Rogava et al., *A&A* **408**, 401 (2003).
 - [7] J. Feys and S.A. Maslowe, *J. Fluid Mech.* **803**, 556 (2016);
 - [8] P. Billant and F. Gallaire, *J. Fluid Mech.* **734**, 5 (2013).
 - [9] K.S. Eckhoff and L. Storesletten, *J. Fluid Mech.* **89**, 401 (1978); K.S. Eckhoff, *J. Fluid Mech.* **145**, 417 (1984).
 - [10] S. Leibovich and K. Stewartson, *J. Fluid Mech.* **126**, 335 (1983).
 - [11] J.T. Ault et al., *Phys. Rev. Lett.* **117**, 084501 (2016).
 - [12] O. Lucca-Negro and T. O'Doherty, *Progr. Energ. Combust. Sci.* **27**, 431 (2001).
 - [13] D.F. Ollis, E. Pelizzetti, and N. Serpone, *Environ. Sci. Technol.* **25**, 1523 (1991).
 - [14] J.R. Lamarsh and A.J. Baratta, *Introduction to Nuclear Engineering*, Prentice Hall 2001.
 - [15] R. MacAndrew et al., *Oilfield Rev.* **5**, 15 (1993).
 - [16] M. Lappa, *Rotating Thermal Flows in Natural and Industrial Processes*, Wiley 2012.
 - [17] F. Kreith, *Adv. Heat Transf.* **5**, 129 (1968); Y.N. Lee and W.J. Minkowycz, *Int. J. Heat Mass Transf.* **32**, 711 (1989); M. Fénot et al., *Int. J. Therm. Sci.* **50**, 1138 (2011); F. Seibold, P. Ligrani, and B. Weigand, *Int. J. Heat Mass Transf.* **187**, 122455 (2022).
 - [18] G. Dhanaraj, K. Byrappa, W. Prasad and M. Dudley (Eds), *Handbook of Crystal Growth*, Springer 2010.
 - [19] C. Vivès, *Int. J. Heat Mass Transf.* **33**, 2047 (1988).
 - [20] D. Takeuchi and D. Jankowski, *J. Fluid Mech.*, **102**, 101 (1981).
 - [21] A. Meseguer and F. Marques, *J. Fluid Mech.* **455**, 129 (2002); *Phys. Fluids*, **17**, 094104 (2005).
 - [22] D. Cotrell and A. Pearlstein, *J. Fluid Mech.* **509**, 331 (2004); D.L. Cotrell and G.B. McFadden, *Phys. Fluids* **17**, 114102 (2005).
 - [23] H. Lüdwig, *Z. Flugwiss.* **12**, 304 (1964).
 - [24] B.S. Ng and E.R. Turner, *Proc. R. Soc. A* **382**, 83 (1982).
 - [25] M. Ali and P. Weidman, *Phys. Fluids* **A5**, 1188 (1993).
 - [26] A. Meseguer and F. Marques, *J. Fluid Mech.*, **402**, 33 (2000).
 - [27] H.A. Snyder and S.K.F. Karlsson, *Phys. Fluids* **7**, 1696 (1964).
 - [28] M. Ali and P. Weidman, *J. Fluid Mech.* **220**, 53 (1990).
 - [29] V. Lepiller et al., *Eur. Phys. J. B* **61**, 445 (2008); H.N. Yoshikawa, M. Nagata, and I. Mutabazi, *Phys. Fluids* **25**, 114104 (2013); R. Guillerm et al., *Phys. Fluids* **27**, 094101 (2015); C. Kang, K.-S. Yang, and I. Mutabazi, *J. Fluid Mech.* **771**, 57 (2015); *Proc. R. Soc. A* **381**, 2022117 (2023).

- [30] B. Eckhardt and D. Yao, *Chaos, Solit. Fract.*, **5**, 2073 (1995).
- [31] O.N. Kirillov and I. Mutabazi, *J. Fluid Mech.* **818**, 319 (2017).
- [32] A. Meyer, I. Mutabazi, H.N. Yoshikawa, *Phys. Rev. Fluids* **6**, 033905 (2021).
- [33] A. Maeder et al., *A&A* **553**, A1 (2013); R.W. Dymott et al., *Mon. Not. R. Astron. Soc.*, **524**, 2857 (2023).
- [34] M.R. Petersen, K. Julien, and G.R. Stewart, *Astrophys. J.* **658**, 1236 (2007); H. Klahr and A. Hubbard, *Astrophys. J.* **788**, 21 (2014); L.E. Held and H.N. Latter, *Mon. Not. R. Astron. Soc.* **480**, 4796 (2018); O.N. Kirillov and F. Stefani, *Phys. Rev. Lett.* **111**, 061103 (2013); F. Stefani and O.N. Kirillov, *Phys. Rev. E*, **92**, 051001 (2015); Y. Wang et al., *Phys. Rev. Lett.* **129**, 115001, (2022).
- [35] S. Masuda, S. Fukuda, and M. Nagata, *J. Fluid Mech.* **603**, 189 (2008); C.J. Heaton, *J. Fluid Mech.* **610**, 391 (2008).
- [36] K. Deguchi and M. Nagata, *J. Fluid Mech.* **678**, 156 (2011).
- [37] A. Bahloul, I. Mutabazi, and A. Ambari, *Eur. Phys. J. AP* **9**, 253 (2000); V. Lepiller et al., *Phys. Fluids* **19**, 054101 (2007).
- [38] C.-C. Wang and F. Chen, *Phys. Fluids* **34**, 104102 (2022).
- [39] S. Leblanc and A. Le Duc, *J. Fluid Mech.* **537**, 433 (2005).
- [40] S. Friedlander and M.M. Vishik, *Phys. Rev. Lett.* **66**, 2204 (1991); D. Ionescu-Kruse, *Phil. Trans. R. Soc. A* **376**, 20170090 (2017).
- [41] O.N. Kirillov, F. Stefani, and Y. Fukumoto, *J. Fluid Mech.* **760**, 591 (2014); O.N. Kirillov, *Proc. R. Soc. A* **473**, 20170344 (2017); J. Labarbe and O.N. Kirillov, *Phys. Fluids*, **33**, 104108 (2021).
- [42] V.P. Maslov, *Russ. Math. Surv.*, **41**(6), 23 (1986).
- [43] P. Hartman and A. Wintner, *Am. J. Math.* **75**, 142 (1958)
- [44] P.G. Drazin, *Introduction to Hydrodynamic Stability*, Cambridge University Press 2002.
- [45] B. Dubrulle et al., *A&A* **429**, 1 (2005).
- [46] A.P. Willis and C.F. Barenghi, *A&A* **388**, 688 (2002); O.N. Kirillov, D.E. Pelinovsky, and G. Schneider *Phys. Rev. E*, **84**, 065301 (2011); O.N. Kirillov and F. Stefani, *Phys. Rev. E*, **84**, 036304 (2011).